Irreducible Solid Electrolytes

New Perspectives on Stabilizing High-Capacity Anodes in Solid-State Batteries

Zhao, Wenxuan; Lavrinenko, Anastasia K.; Tu, Meng fu; Huet, Lucas; Vasileiadis, Alexandros; Famprikis, Theodosios; Wagemaker, Marnix; Ganapathy, Swapna

DOI
10.1021/acsenergylett.5c02289

Publication date
2025

Document Version
Final published version

Published in
ACS Energy Letters

ACS Energy Letters

http://pubs.acs.org/journal/aelccp

PERSPECTIVE

Irreducible Solid Electrolytes: New Perspectives on Stabilizing High-Capacity Anodes in Solid-State Batteries

Wenxuan Zhao,[†] Anastasia K. Lavrinenko,[†] Meng-fu Tu, Lucas Huet, Alexandros Vasileiadis, Theodosios Famprikis, Marnix Wagemaker,* and Swapna Ganapathy*

Cite This: *ACS Energy Lett.* 2025, 10, 5363−5372

ABSTRACT: **Irreducible solid electrolytes (SEs), characterized by non-Li framework ions in their lowest oxidation states, offer intrinsic compatibility with low-reduction-potential, high-capacity negative electrodes, such as lithium metal and silicon. In these SE materials, disorder engineering and vacancy formation reduce lithium-ion diffusion barriers, achieving room-temperature ionic conductivities exceeding 0.1 mS cm^{-1}. Experiments and atomistic simulations confirm that irreducible SEs form decomposition-free interfaces with Li metal. Their limited oxidative stability can be addressed by pairing them with an electrolyte layer stable with practical cathodes yet demanding interface compatibility between the two electrolyte layers. Here we highlight key research directions to accelerate irreducible SE transition from laboratory to practical application, including expanding compositional diversity, optimizing interfaces with cathode-facing electrolytes, developing scalable thin-film processing, and exploring compatibility with other low working potential anodes like silicon. Addressing these challenges is essential to unlock the full potential of irreducible SEs for high-energy, long-life, all-solid-state batteries.**

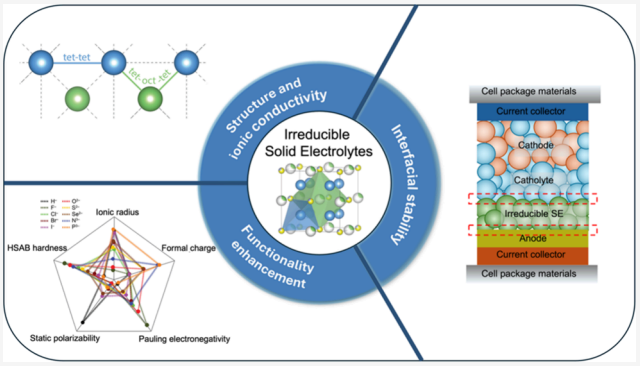

All-solid-state batteries (ASSBs) promise safe, high-energy density storage by pairing high-capacity anodes with nonflammable ceramic solid electrolytes (SEs).[1] Their gravimetric energy density could exceed 350 Wh kg^{-1} (ref 2), and removal of liquid electrolytes raises the onset temperature of thermal runaway,[3,4] positioning ASSBs at the forefront of next-generation battery research.

These expectations put high demands on the properties of the SEs, i.e., liquid-like ionic conductivities (≥1 mS cm^{-1}) and electrochemical stability across the full-cell voltage. Oxyhalides[5,6] (e.g., $LiTaOCl_4$) and halogen-rich argyrodites[7−10] (e.g., $Li_{5.3}PS_{4.3}Br_{1.7}$) already achieve conductivities of ∼10 mS cm^{-1}, yet their electrochemical stability window (ESW) is limited, owing to fragile anionic (e.g., S^{2-}) or cationic frameworks (e.g., Ta^{5+}, P^{5+}) upon oxidation or reduction, respectively.[11,12] While high-potential-tolerant halide SEs[13−15] and protective coatings[16] improve electrochemical compatibility at the positive electrode, their development and application at the negative electrode remain challenging.

Li metal and Si-based anodes achieve exceptional capacities but demand (electro)chemical passivation down to ∼0 V vs Li/Li$^+$.[17,18] However, common SEs, such as sulfides, oxides, and halides, typically reduce to low-valence states or even elemental metals at low potentials.[11] If the resulting products are mixed ion-electron conductors, reduction can propagate, leading to continuous SE decomposition.[19] Certain SEs, such as sulfur-based argyrodites,[20] lithium phosphorus oxynitride (LiPON)[19] and hydrides,[21] instead exhibit kinetic stability by forming electronically insulating and self-limiting interphases. For example, Li_6PS_5Cl decomposes into poorly electronconductive products such as LiCl, Li_2S, and Li_3P,[12] while $LiBH_4$-$[LiNBH]_n$ systems generate passivation layers of Li−B and Li_3N[22] in situ. Although such interphases suppress further decomposition, they inevitably increase interfacial resistance and consume active Li,

Received: July 22, 2025
Revised: September 15, 2025
Accepted: September 24, 2025

https://doi.org/10.1021/acsenergylett.5c02289
ACS Energy Lett. 2025, 10, 5363−5372

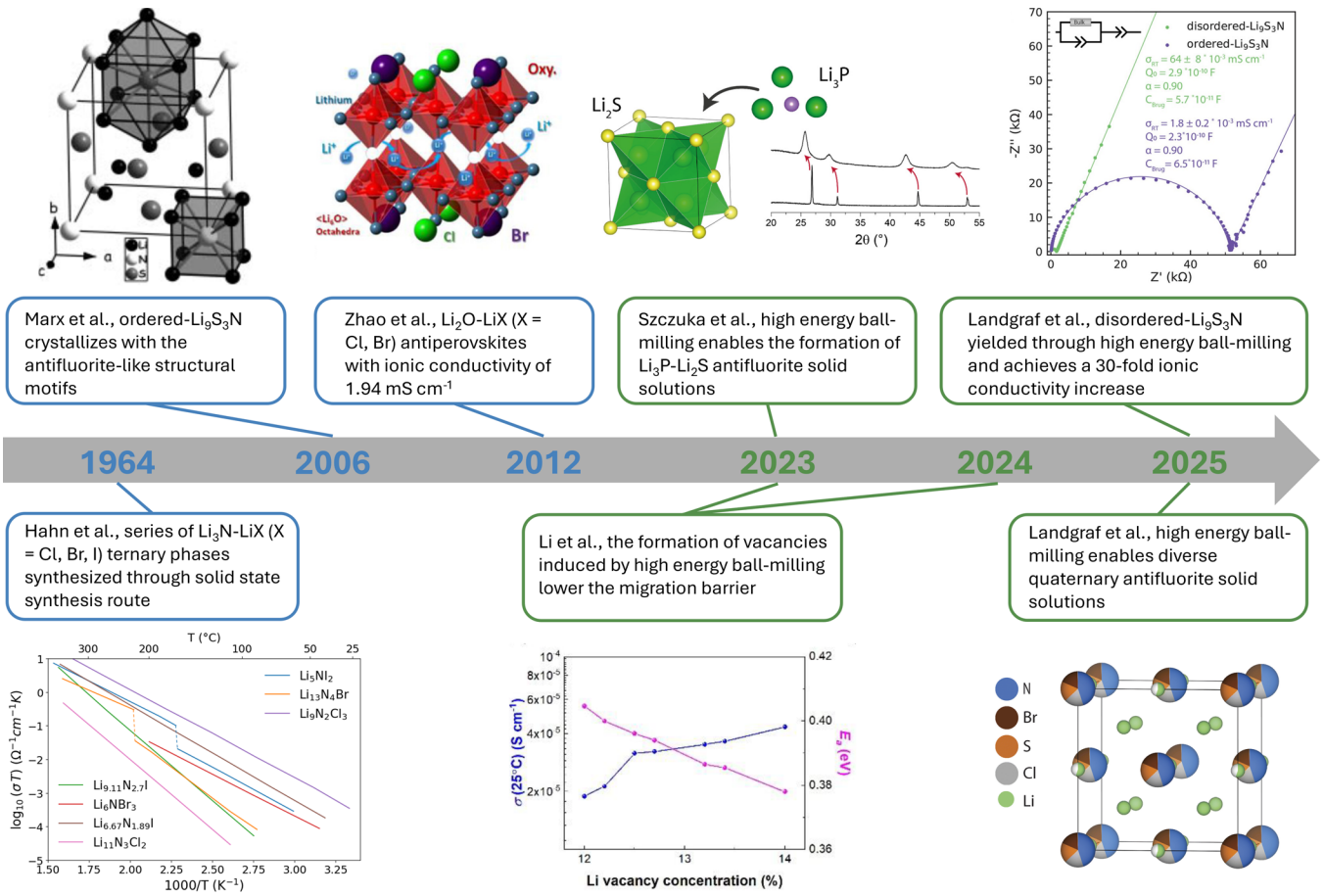

Figure 1. Timeline of the development of irreducible SE families. Adapted with permission from ref 31. Copyright 1981 Elsevier. Reprinted with permission from ref 32. Copyright 2006 Wiley-VCH Verlag GmbH & Co. KGaA. Reprinted with permission from ref 23. Copyright 2012 American Chemical Society. Reprinted with permission from ref 28. Copyright 2023 American Chemical Society. Reprinted with permission from ref 24. Available under a CC BY-NC 4.0. Copyright 2023 American Association for the Advance of Science. Reprinted with permission from ref 29. Copyright 2024 Springer Nature. Reprinted with permission from ref 27. Available under a CC-By 3.0. Copyright 2025 Royal Society of Chemistry. Reprinted with permission from ref 26. Copyright 2025 American Chemical Society.

often necessitating prelithiation strategies to compensate for the associated Li loss.

Comparably, an evident strategy to mitigate anode-side instability is to design SEs that are inherently stable against low-potential anodes. This requirement is fulfilled if all elements of the SE, except for Li-ions, are in their lowest oxidation state and thus irreducible (e.g., the lithium binaries LiX with X = N^{3-}, O^{2-}, S^{2-}, Cl^{-}). Recent advances have expanded the landscape of such irreducible SEs, including antifluorite-type materials like Li_3N-LiX (X = Cl, Br), Li_3N-Li_2S, Li_3P-Li_2S and antiperovskites[17,23−28] (Figure 1).

Mechanochemical synthesis introducing structural and compositional disorder has substantially boosted their room-temperature ionic conductivities.[26−28] As intended, these materials exhibit excellent electrochemical stability down to ∼0 V vs Li/Li^+ and show no reactivity or solid electrolyte interface (SEI) formation upon direct contact with Li metal.[17,25,29,30] Practical cell application, however, also demands oxidative stability during delithiation of the anode (e.g., up to ∼1 V vs Li/Li^+ for silicon[18]) and interfacial compatibility with the positive electrode. Since the oxidative stability of current irreducible SEs is inherently limited, the solution is paring them with a catholyte (cathode-facing electrolyte) yet introducing new interface compatibility challenges.

In this Perspective, we critically assess recent experimental and computational advancements in irreducible SEs, identify prevailing challenges, and outline key research directions aimed at fully exploiting their potential and enabling their transition from lab materials to practical application in next-generation ASSBs.

The most well-known irreducible compounds are lithium binaries such as lithium halides (e.g., LiCl), chalcogenides (e.g., Li_2S), and pnictides (e.g., Li_3N). Since the 1960s, the solid-state synthesis route, in which the reactants are annealed under high temperature, has yielded numerous ternary phases along the Li_3N-LiX (X = Cl, Br, I) tie line[31] (Figure 1). Later, similar methods led to the discovery of ternary compounds in the Li_3N-Li_2S[32] and Li_2O-LiX[23] systems. However, only select compounds like α-Li_3N (hexagonal $P6/mmm$)/β-Li_3N (antifluorite),[29] Li_7N_2I,[33] and certain antiperovskites[23] exhibit room-temperature ionic conductivities above 0.1 mS cm^{-1}, hindering practical application. Moreover, reported conductivities differ by more than an order of magnitude for the latter two compounds, underscoring reproducibility challenges.[34,35]

Among the emerging families of irreducible SEs antifluorite-type phases have recently attracted considerable attention due to their ionic conductivities achieving ∼1.0 mS cm^{-1} and inherent structural and compositional flexibility, which can further enhance lithium-ion diffusion. In addition, many recent studies

https://doi.org/10.1021/acsenergylett.5c02289
ACS Energy Lett. 2025, 10, 5363−5372

have investigated ionic transport, the role of disorder, and electrochemical stability within antifluorites,[17,24−27,36] motivating the focus on this motif as a representative case study.

In the anion-disordered lithium-rich antifluorite structure (Figure 2a), Li^+ primarily occupies tetrahedral sites (Li-tet),

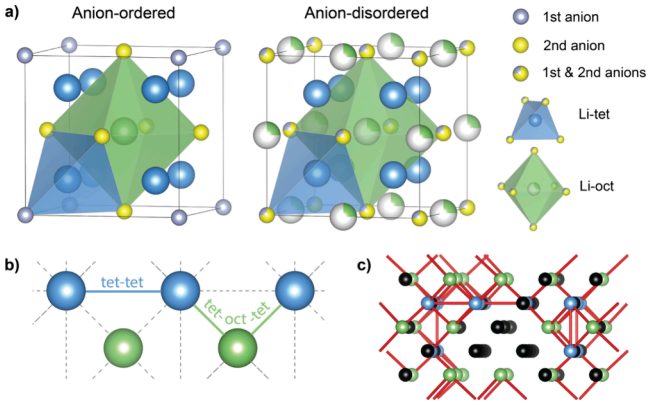

Figure 2. Structure and ion transport in lithium-rich irreducible antifluorite SEs. (a) Ordered and disordered configurations in a ternary compound with two anion species (e.g., S^{2-} and N^{3-}). Lithium occupies tetrahedral (blue) and octahedral (green) sites, while anions are shown in yellow and violet. (b) The two primary lithium migration pathways. (c) Example of a percolation network, where active tetrahedral (blue) and octahedral (green) lithium sites form a continuous conduction pathway (connected by red jumps), while isolated Li sites (black) remain disconnected at the chosen energy cutoff.

while energetically less favorable octahedral sites (Li-oct) are only partially occupied. Density functional theory (DFT) and *ab initio* molecular dynamics (AIMD) identify two main migration pathways (Figure 2b): (1) direct hopping between tetrahedral sites (tet-tet) and (2) via interstitial octahedral positions (tet-oct-tet).[26,27,30]

Compositional and structural disorder can stabilize these high-energy octahedral sites, widen diffusion bottlenecks and create low-energy pathways for long-range diffusion by introducing diversity of local environments. For example, partial substitution of larger anions (e.g., Cl^- or S^{2-}) with smaller ions (e.g., N^{3-}) enlarges diffusion bottlenecks,[26,27] while introducing larger anions (e.g., Br^- instead of Cl^- in $Li_{2.31}S_{0.41}Br_{0.14}N_{0.45}$) increases lattice parameters and polarizability,[27] both relieving steric constraints for ion migration. Substitution with higher oxidation state anions (e.g., S^{2-} with P^{3-}) increases lithium content and modifies Coulombic interactions in the system, stabilizing octahedral Li sites and reducing migration energy barriers.[30] Anion-disordered arrangement (e.g., N^{3-} and S^{2-} sharing the same crystallographic position) diversifies local coordination environments, creating energetically favorable diffusion pathways absent in anion-ordered configurations (Figure 2a). The percolation model further demonstrates that compositional and structural disorder in $Li_{2+x}S_{1-x}N_x$ exhibits a lower percolation-onset energy and a higher fraction of lithium ions connected to the percolation network (Figure 2c illustrates an example of percolation network), thereby enhancing ionic conductivities.[26] Compositional and structural disorder, typically introduced through mechanochemical synthesis, effectively lowers the Li-ion diffusion energy barrier and, in turn, boost the ionic conductivity of irreducible antifluorite SEs.

> Compositional and structural disorder, typically introduced through mechanochemical synthesis, effectively lowers the Li-ion diffusion energy barrier and, in turn, boost the ionic conductivity of irreducible antifluorite SEs.

To obtain these metastable and highly disordered phases, irreducible antifluorite SEs are typically synthesized through mechanochemistry instead of traditional high-temperature solid-state routes.[26] Along the $LiCl-Li_3N$, Li_2S-Li_3N, Li_2S-Li_3P, and $LiX-Li_2S-Li_3N$ (X = Cl, Br) tie lines, this approach has yielded a diverse range of disordered ternary and quaternary solid solutions with enhanced ionic conductivities (Figure 1). For example, high-energy milling induces structural disorder in $Li_{2+x}S_{1-x}N_x$, resulting in orders of magnitude increase in ionic conductivity from 0.002 to 0.2 mS cm^{-1} (ref 26). In β-Li_3N[29] and $Li_9N_2Cl_3$,[24] it has been proposed that high-energy ball-milling provides the energy required to create lithium and nitrogen vacancies that lower the diffusion barrier and increase ionic conductivity by an order of magnitude.

The largely unexplored chemical space and high structural flexibility of irreducible antifluorite SEs allow to tune the atomic scale interactions that govern ion transport. As a result, this class of materials provides future opportunities to systematically explore structure-performance relationships and to design novel irreducible SEs for next generation ASSBs. The high structural flexibility of irreducible antifluorite SEs offer a promising opportunity to simultaneously enhance ionic conductivity and electrochemical stability through rational selection of anions.

> The high structural flexibility of irreducible antifluorite SEs offer a promising opportunity to simultaneously enhance ionic conductivity and electrochemical stability through rational selection of anions.

Reversible cycling of high-energy-density ASSBs requires stable electrode|SE interfaces across the full cell voltage, thus demanding a SE with a sufficiently wide ESW to cover the working potentials of both electrodes. This prevents undesirable redox reactions, Li inventory loss, and increased impedance induced by less conductive decomposition products.[37] Li metal presents the most stringent negative electrode active material for reduction stability, featuring the lowest standard reduction potential for Li^+ (−3.04 V vs standard hydrogen electrode).[17] Typical oxidation potentials exceed 4 V vs Li/Li^+ depending on the precise choice of the positive electrode active material.

A rapid and cost-effective approach to estimate ESW of SEs is to employ atomistic simulations.[38] For irreducible binaries such as Li_3N and Li_2S, thermodynamic calculations based on the decomposition products predict a stability down to 0 V vs Li/Li^+, confirming their intrinsic compatibility with Li metal anodes.[39] Similarly, the grand-potential phase diagram shows that $Li_{2.5}N_{0.5}S_{0.5}$ remains thermodynamically stable at 0 V vs Li/Li^+ (Figure 3a),[17] unlike commonly studied sulfides, halides, oxides, and LIPON-type SEs which tend to get reduced.[40] Experimental cyclic-voltammetry (CV) scans of symmetric $Li|Li_{2+x}S_{1-x}N_x|Li$

https://doi.org/10.1021/acsenergylett.5c02289
ACS Energy Lett. 2025, 10, 5363−5372

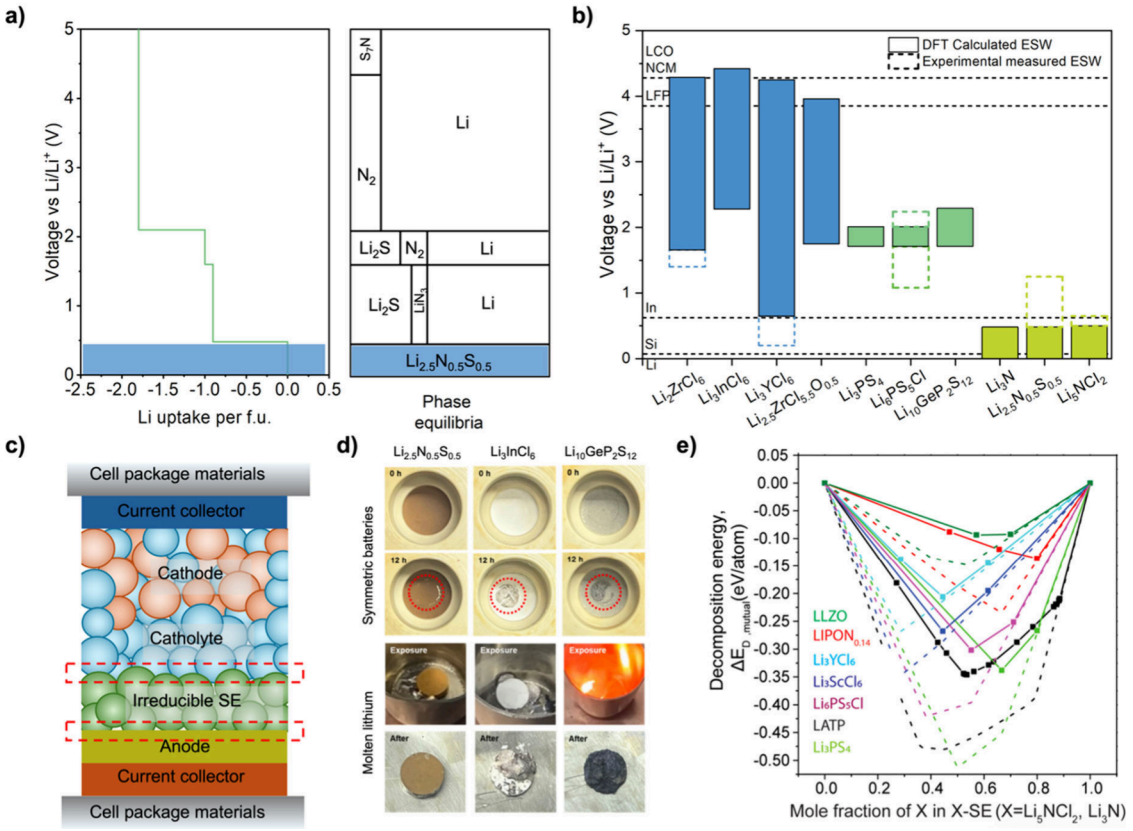

Figure 3. Interfacial stability of irreducible SEs. (a) Grand-potential phase diagram and equilibrium voltage profile of $Li_{2.5}N_{0.5}S_{0.5}$. The blue part denotes the thermodynamic stability down to 0 V vs Li/Li^+. Adapted with permission from ref 17. Copyright 2024 American Chemical Society. (b) ESWs for representative SEs, reported in the literature:[11,17,26,27,29,39,41,42] solid bars indicate first-principles predictions; open bars show voltametric measurements. The dashed lines indicate the typical reduction limit of anodes and oxidation limit of cathodes. (c) Schematic illustration of an anode|irreducible SE|catholyte|cathode stack configuration. (d) Optical images of SE pellets before testing, after 12 h of aging in Li|SE|Li symmetric cells, and after being exposed to molten Li. Reprinted with permission from ref 17. Copyright 2024 American Chemical Society. (e) Reaction energies for pseudobinary mixtures of Li_5NCl_2 (solid line) and Li_3N (dashed line) with several highly conducting SEs. Reprinted with permission from ref 25. Copyright 2023 American Chemical Society.

cells further show no reduction peaks down to 0.1 V vs Li/Li^+, corroborating their electrochemical irreducibility.[26]

As summarized in Figure 3b, irreducible SEs consistently exhibit excellent reduction stability, aligning with their chemistry-by-design principle (fully reduced anions). However, their oxidative stability is inherently limited. Phase-stability calculations predict the oxidation limits of ~0.5 V vs Li/Li^+ for Li_3N, Li_3N−LiCl and Li_3N−Li_2S.[17,25,39] Although experimental linear sweep voltammetry (LSV) measurements revealed extended oxidation stability limits of ~0.65 V for Li_3N−LiCl[27] and ~2 V for Li_3N−Li_2S,[26] these values are still insufficient for directly pairing with ≥4 V cathodes. Notably, computational ESW estimations, based on the total energy of reactant SE and decomposition products, account only for the thermodynamic driving forces and neglect kinetic barriers, typically underestimating the ESW. By incorporating the kinetic stability into the ESW analysis, wider stability limits are often predicted, showing good agreement with experimental stability data across diverse classes of SEs[38] and even predicting the limits of reversible (de)lithiation.[11] Therefore, further experimental and theoretical studies remain essential to fully understand and optimize the oxidative stability of irreducible SEs.

Given that oxidation-induced degradation remains a challenge at high potentials for current irreducible SEs, a promising engineering solution is to employ a bilayer configuration. Recent studies have demonstrated that bilayer designs can suppress interfacial degradation, broaden the ESW, and enable long-term cycling.[43] For example, pairing an argyrodite catholyte with a hydride-based anolyte $Li_5PS_4(BH_4)_2$ enhances interfacial stability toward Li metal and delivers longer cycling than cells with Li_6PS_5Cl alone.[44] Translating this concept into irreducible SEs, one could envision integrating a more oxidatively robust halide or sulfide catholyte to stabilize the high-potential interface (i.e., an irreducible SE|catholyte bilayer, as illustrated in Figure 3c). In this way, the irreducible SE would only need to remain stable above the catholyte's reduction potential (e.g., 0.6 V for Li_3YCl_6[45] or 1.08 V for Li_6PS_5Cl[11]), thereby relaxing the oxidative stability requirement for irreducible SEs while leveraging its intrinsic reduction stability at the anode side.

Although an irreducible SE|catholyte bilayer stack can theoretically secure a desired ESW that spans the full-cell operation voltage, ESW alone does not guarantee interfacial compatibility and cycling durability. The chemical stability of the SE with adjacent components (e.g., anode and pairing catholyte chemistries), as well as cycle performance of the resulting bilayer electrolyte, are equally critical.

Recent studies have investigated the cyclability of irreducible SE layers such as Li_3N and Li_3OCl, significantly suppressing interfacial degradation and broadening ESW when paired with

https://doi.org/10.1021/acsenergylett.5c02289
ACS Energy Lett. 2025, 10, 5363−5372

cathode-stable electrolytes. Applying an ultrathin Li_3N coating on garnet-type LLZO reduces initial interfacial resistance by more than an order of magnitude, enabling stable operation for hundreds of hours in Li|Li symmetric cells and over 400 stable cycles in Li|$LiFePO_4$ full-cells.[11,46] Likewise, a Li_3OCl coating on argyrodite suppresses electron penetration and lithium dendrite growth, delivering higher current density, longer cycle life, and superior rate capability compared to bare Li_6PS_5Cl in both symmetric and full cells.[47] Similar improvements are observed when irreducible SE interlayers separate Li metal from halide or sulfide electrolytes, markedly extending cycle life.[48−51]

Notably, stable cycling does not necessarily indicate chemical compatibility. For example, sulfide-based SEs such as Li_6PS_5Cl rapidly form passivating layers at the Li metal[20] interface, masking ongoing decomposition. Therefore, to assess true (electro)chemical stability, it is important to combine electrochemical measurements with in situ or post-mortem structural, chemical, and morphological analyses, supported by atomic-scale simulations of interfacial reactivity at both anode and catholyte interfaces.[17,24,29]

Direct optical and spectroscopic measurements confirm that irreducible SEs remain inert to Li metal. Yu et al. observed no apparent color change in the Li|$Li_{2.5}N_{0.5}S_{0.5}$|Li pellet after 12h of open-circuit aging (Figure 3d). Further exposing $Li_{2.5}N_{0.5}S_{0.5}$ to molten Li resulted in neither detectable visual changes nor new phase formation, as confirmed by X-ray photoelectron spectroscopy.[17] Similarly, post-mortem analysis of β-Li_3N after cycling, using high-resolution scanning electron microscopy, X-ray absorption near edge structure, and scanning transmission X-ray microscopy, demonstrated no morphological or chemical degradation.[29]

To support experimental observations, AIMD simulations can provide atomic-scale insights into chemical stability and kinetic reactivity at the interfaces. For example, an Li_5PS|Li interface remained stable during 100 ps of AIMD. Although this is very short compared to practical time scales, reducible electrolytes $Li_7P_3S_{11}$ and Li_3PS_4 under the same conditions showed rapid SEI layer growth, driven by the dissolution of PS_4^{3-} and $P_2S_7^{4-}$ units.[30] Similarly, AIMD simulations of $Li_9N_2Cl_3$|Li interface showed no SEI formation or interfacial reactivity consistent with the anticipated electrochemical stability of $Li_9N_2Cl_3$ toward Li metal.[52]

To assess chemical stability at interfaces between irreducible SEs (Li_3N and Li_5NCl_2) and catholytes, Landgraf et al. employed a pseudobinary model[25] (Figure 3e). The calculations showed significantly lower thermodynamic driving forces for decomposition in contact with garnet (LLZO), LIPON-type, and halide catholytes compared to sulfide or lithium aluminum titanium phosphate (LATP) SEs. Follow-up experiments confirmed stable Li_3N|Li_3YCl_6 interface with no new phases and minimal interfacial resistance change during prolonged cycling.[29] Combining irreducible SEs with cathode-stable electrolytes addresses oxidative stability challenges, but achieving true interface compatibility and long-term cycling performance necessitates integrated electrochemical characterization, advanced in situ or post-mortem analysis, and atomic-level simulations of interfacial reactions at both anode and catholyte interfaces.[29]

Although systematic studies remain sparse, pairing irreducible SEs with cathode-stable electrolytes (e.g., garnet, LIPON, sulfide or halide SEs) clearly mitigates intrinsic oxidative stability limitations. Catholyte selection principles should be guided by (i) high oxidative stability to protect the cathode interface, (ii) fast Li-ion conductivity to mitigate transport bottlenecks, and (iii) thermodynamic and kinetic compatibility with irreducible SEs to prevent undesirable reactions. Halide catholytes such as Li_3YCl_6 and Li_3InCl_6 are particularly promising because of their high oxidative stability (>4.5 V) and relatively wide ESW, while sulfide catholytes like Li_6PS_5Cl offer excellent ionic conductivity (>10^{-3} S cm^{-1}) and good processability. Further systematic research focusing on interfacial stability and long-term cycling remains crucial to facilitate the practical application of irreducible SEs.

Combining irreducible SEs with cathode-stable electrolytes addresses oxidative stability challenges, but achieving true interface compatibility and long-term cycling performance necessitates integrated electrochemical characterization, advanced in situ or post-mortem analysis, and atomic-level simulations of interfacial reactions at both anode and catholyte interfaces.

Although the ionic conductivity and anode stability have advanced markedly, several aspects must still be addressed before irreducible SEs can be applied in practical systems. These include air stability and large-scale manufacturing of thin layers.

The anion framework of irreducible SEs typically comprises P^{3-}, N^{3-}, or S^{2-}, which readily hydrolyze upon exposure to moisture, resulting in material decomposition, toxic gas evolution, and loss of ionic conductivity.[53−56] Consequently, irreducible SE powders and films must be sufficiently stable under standard dry-room conditions to avoid the need for costly inert-atmosphere processing. Some nitride-based irreducible SEs remain stable under dry air, yet even trace humidity compromises their structure and conductivity.[57] For example, vacancy-rich $Li_9N_2Cl_3$ is stable at ∼3−5% relative humidity (RH) but degrades at ambient conditions (≈20% RH), forming $Li_4(OH)_3Cl$ and NH_3.[24] Likewise, β-Li_3N preserves its structure in dry air but rapidly acquires a self-passivating LiOH layer under modest moisture conditions.[29] Although these cases suggest that today's industrial dry rooms (<1% RH) are adequate for manufacturing irreducible SEs, a deeper understanding of moisture-induced degradation mechanisms and the design of intrinsically air-stable compounds remains essential.

Another critical factor for practical implementation is the gravimetric energy density which scales with both electrolyte's density and its thickness. The irreducible SEs considered here (e.g., ρ_{Li_3N} = 1.27 g cm^{-3}; $\rho_{Li_{2.5}N_{0.5}S_{0.5}}$ = 1.63 g cm^{-3}; $\rho_{Li_9N_2Cl_3}$ = 1.7 g cm^{-3})[24,26,29] have densities comparable to, or even lower than common sulfide ($\rho_{Li_6PS_5Cl}$ = 1.8 g cm^{-3})[58] and halide ($\rho_{Li_6YCl_3}$ = 2.1 g cm^{-3})[59] SEs. Thus, at a given thickness, these irreducible SEs do not inherently reduce energy density relative to common alternatives. Electrolyte thickness is equally important: thick electrolyte layers not only add mass, thereby lowering energy density, but also significantly increase cell impedance and overpotential.[60] Irreducible SEs achieve conductivities of 0.1 mS cm^{-1}, yet this is still 2 orders of magnitude below leading sulfide electrolytes.[26,27] Therefore, minimizing SE layer thickness is imperative to maintain acceptable ohmic losses at practical C-rates. Cold-pressed laboratory pellets typically measure several

https://doi.org/10.1021/acsenergylett.5c02289
ACS Energy Lett. 2025, 10, 5363−5372

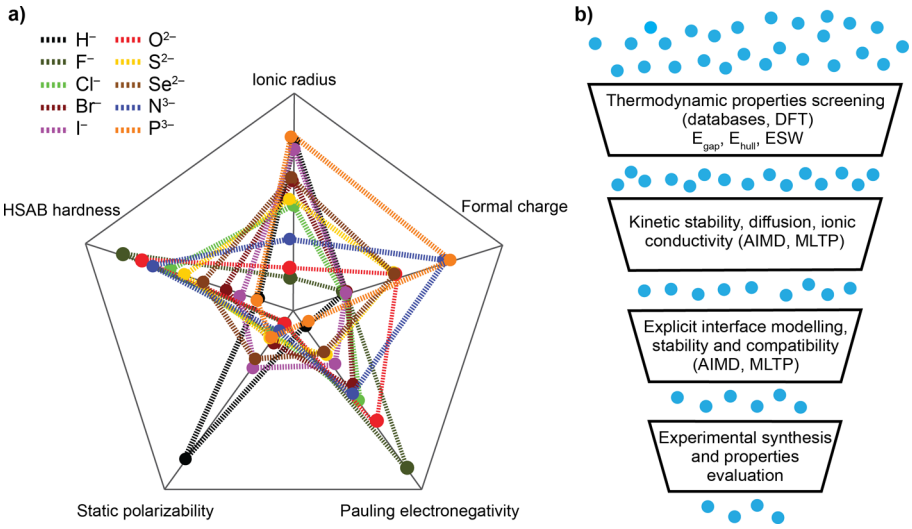

Figure 4. Screening and optimization strategies for irreducible SE design. (a) Key anion properties including ionic radius, formal charge, electronegativity, polarizability, and chemical hardness. (b) Schematic overview of computational screening workflow integrating DFT, MD, and machine learning (ML) techniques like ML trained potentials (MLTPs) to identify promising irreducible SE candidates.

hundred micrometers, far above the <30 μm target for high-energy, fast-charge batteries.[2,61] Scalable roll-to-roll methods (e.g., tape casting, extrusion, and dry calendaring[62−64]) can achieve smaller thicknesses, but the binders and solvents involved in these processes may chemically react with irreducible SEs.[65,66] Alternative additive-free methods (e.g., electrodeposition[46] and atomic-layer deposition[67]) yield sub-micrometer films which renders them more prone to fail from short circuit due to lithium dendrite formation. Indeed, Li filament penetration depths of 2−10 μm have been reported for Li_3N−LiF[49] and Li_7N_2I[33] interlayers after only ∼50 cycles. These findings underscore the need to suppress dendrite formation.

Thus, optimizing irreducible SEs for industrial applications demands simultaneous improvement in ionic conductivity, electrochemical stability, and mechanical resilience. Intrinsic anion properties, such as ionic radius, formal charge, electronegativity, polarizability, and chemical hardness (Figure 4a), offer useful guiding principles directly influencing diffusion and stability of irreducible SEs. For example, ionic radius and formal charge tune diffusion bottleneck size and Li^+−anion Coulombic interactions.[27] Larger, lower-charge anions (e.g., S^{2-}) widen diffusion pathways, whereas smaller, highly charged anions (e.g., N^{3-}) increase lithium concentration and introduce favorable structural disorder, accelerating ionic transport.[26,68] Electronegativity sets the valence-band depth and therefore oxidative stability.[45] Highly electronegative O^{2-} and F^- deepen the valence band and harden the lattice,[69] whereas less electronegative ions (e.g., S^{2-}) trade some oxidative robustness for faster Li^+ mobility.[70] The combined influence of polarizability and electronegativity is captured by ionization potential trends, which empirically rank binary irreducible SEs for oxidative stability ($N^{3-} < P^{3-} < H^- \ll S^{2-} < I^- < O^{2-} < Br^- < Cl^- \ll F^-$).[39] Recent work on $Li_{2.65}S_{0.35}N_xP_{0.65-x}$ solid solutions illustrates how systematic and targeted anion substitution can exploit these trends to simultaneously enhance ionic conductivity and oxidative stability.[68] Compared to reported irreducible SE families, this material achieves a standout ionic conductivity (>1 mS cm^{-1}) coupled with an extended oxidation stability (1.15 V vs Li^+/Li), enabling compatibility not only with Li but also within composite Si anodes. Although its chemo-mechanical compatibility during Si volume changes remains underexplored, this study provides a compelling example of how anion engineering within the antifluorite framework can balance ionic transport with stability. Moreover, polarizability and chemical hardness also govern lattice softness and air robustness,[70,71] yet their influence on irreducible SEs remains largely unexplored. So far, only a handful of ternaries (and even fewer quaternary) compounds have been investigated, leaving an expansive compositional space unprobed. Although irreducible SEs have mostly been explored with lithium metal anodes, they also hold significant promise for forming stable, SEI-free interfaces with alternative high-capacity anodes such as silicon, provided their electrochemical stability extends beyond 1 V vs Li/Li^+ during cycling.

Although irreducible SEs have mostly been explored with lithium metal anodes, they also hold significant promise for forming stable, SEI-free interfaces with alternative high-capacity anodes such as silicon, provided their electrochemical stability extends beyond 1 V vs Li/Li^+ during cycling.

Investigation of this wide compositional space calls for systematic computational screening (Figure 4b) coupled with targeted synthesis and properties characterization. Computational approaches, including DFT, AIMD, and ML, can rapidly evaluate thermodynamic stability, electronic structure, lattice softness, Li diffusion mechanisms, and bottleneck geometry, thereby flagging promising candidates prior to synthesis.[72−74] High-throughput DFT screening of formation energies, band gaps, above-hull stabilities, ionic conductivities, and reaction energies has already guided the search for Li- and Na-ion conducting SE candidates[73] and compatible coatings for halide SEs.[48] For irreducible SEs, additional prescreening metrics, including bottleneck size, diversity of Li environments, and electrostatic interaction strength, can capture the effects of anion

https://doi.org/10.1021/acsenergylett.5c02289
ACS Energy Lett. 2025, 10, 5363−5372

disorder. Experimental characterization, coupled with explicit interface modeling, is then required to assess chemical reactivity and Li-ion transport across heterointerfaces. To reach larger length and time scales, ML interatomic potentials enable nanosecond-to-microsecond simulations over hundreds of nanometers,[75] which could be sufficient to probe early dendrite formation, optimize coating thickness, and track the initial evolution of SEI —all of which would be practically intractable by AIMD.[76,77]

Irreducible SEs in which all non-lithium elements are already in their lowest oxidation state exhibit intrinsic reduction stability. This property makes them attractive to pair with low-potential, high-capacity anodes such as Li metal and silicon. Their main weaknesses are (i) limited oxidative stability, which requires a cathode-stable protective layer; (ii) sensitivity to ambient moisture despite tolerance to dry-air conditions; and (iii) moderate ionic conductivity (commonly ≤ 0.2 mS cm^{-1}), which requires thin-film processing. To resolve these concerns, we propose the following research directions:

1) Compositional engineering beyond traditional anions: The rational combination of anions with different ionic radii and electronegativity can simultaneously widen diffusion bottlenecks and deepen the valence band, thus improving both conductivity and oxidative stability. Integrating high-throughput DFT, AIMD, and ML potentials will accelerate screening of available vast chemical design space.
2) Investigating interfaces with cathode-stable electrolytes: Pairing irreducible SEs with a cathode-stable layer (e.g., halide or oxide SEs) demands systematic studies of interfacial thermodynamics, Li-ion transport, and redox chemistry both experimentally and through atomic-scale modeling.
3) Expanding application beyond Li metal anodes: While studies have primarily focused on Li metal anodes, irreducible SEs are promising to form decomposition-free interfaces with other high-capacity anodes (e.g., silicon).
4) Scalable thin-film processing: Atomic-layer deposition or electrodeposition can yield submicrometer irreducible SEs coatings required to maintain high-energy density and ionic conductivity.

AUTHOR INFORMATION

Corresponding Authors

Marnix Wagemaker − *Radiation Science and Technology, Faculty of Applied Sciences, Delft University of Technology, Delft 2629 JB, The Netherlands;* orcid.org/0000-0003-3851-1044; Email: m.wagemaker@tudelft.nl

Swapna Ganapathy − *Radiation Science and Technology, Faculty of Applied Sciences, Delft University of Technology, Delft 2629 JB, The Netherlands;* orcid.org/0000-0001-5265-1663; Email: s.ganapathy@tudelft.nl

Authors

Wenxuan Zhao − *Radiation Science and Technology, Faculty of Applied Sciences, Delft University of Technology, Delft 2629 JB, The Netherlands*

Anastasia K. Lavrinenko − *Radiation Science and Technology, Faculty of Applied Sciences, Delft University of Technology, Delft 2629 JB, The Netherlands;* orcid.org/0000-0001-9863-8325

Meng-fu Tu − *Radiation Science and Technology, Faculty of Applied Sciences, Delft University of Technology, Delft 2629 JB, The Netherlands*

Lucas Huet − *Radiation Science and Technology, Faculty of Applied Sciences, Delft University of Technology, Delft 2629 JB, The Netherlands*

Alexandros Vasileiadis − *Radiation Science and Technology, Faculty of Applied Sciences, Delft University of Technology, Delft 2629 JB, The Netherlands;* orcid.org/0000-0001-9761-7936

Theodosios Famprikis − *Radiation Science and Technology, Faculty of Applied Sciences, Delft University of Technology, Delft 2629 JB, The Netherlands;* orcid.org/0000-0002-7946-1445

Complete contact information is available at: https://pubs.acs.org/10.1021/acsenergylett.5c02289

Author Contributions

†W.Z and A.K.L. contributed equally to this work.

Notes

The authors declare no competing financial interest.

Biographies

Wenxuan Zhao is a Ph.D. student in the Storage of Electrochemical Energy group at Delft University of Technology. His research focuses on the design, synthesis, and development of solid electrolytes for advanced anode materials.

Anastasia K. Lavrinenko is a Ph.D. student in the Storage of Electrochemical Energy group at Delft University of Technology. Her research focuses on employing atomic-scale simulations and machine learning methods to investigate the properties of materials and interfaces, as well as on developing analysis tools for molecular dynamics.

Meng-fu Tu is a Ph.D. student in the Storage of Electrochemical Energy group at Delft University of Technology. His research focuses on developing irreducible solid electrolytes and investigating their applications on low-potential anodes.

Lucas Huet is a postdoctoral fellow at Delft University of Technology. He received his Ph.D. in Energy and Materials Sciences and in Materials Chemistry, conjointly from the University of Quebec and the University of Nantes, in 2022. His research focuses on silicon anodes and electrolytes for Li-ion batteries.

Alexandros Vasileiadis is an Assistant Professor at Delft University of Technology, where he leads the computational section of the Storage of Electrochemical Energy (SEE) group. His research focuses on multiscale modeling, ranging from atomic scale to interfacial and mesoscale simulations of materials and energy devices, as well as AI-driven materials discovery.

Theodosios Famprikis is currently a Royal Society Newton International fellow at the University of Oxford, following a Marie-Skłodowska-Curie postdoctoral fellowship at TU Delft. His research encompasses the role of atomic structure and dynamics on the properties of functional materials, with a particular focus on disordered materials for solid-state ionics.

Marnix Wagemaker is a full professor at Delft University of Technology and head of the Storage of Electrochemical Energy group, which focuses on next-generation battery materials. His research combines experimental and theoretical approaches to deepen the fundamental understanding of electrochemical energy storage processes and drive their advancement. Webpage: https://www.tudelft.nl/tnw/over-faculteit/afdelingen/radiation-science-

https://doi.org/10.1021/acsenergylett.5c02289
ACS Energy Lett. 2025, 10, 5363−5372

technology/research/research-groups/storage-of-electrochemical-energy/people/marnix-wagemaker

Swapna Ganapathy is a staff scientist specializing in battery science and solid-state NMR at Delft University of Technology. Her work focuses on employing advanced characterization techniques to investigate interfacial phenomena and elucidate structure−function relationships in inorganic and polymer-based hybrid electrolytes for solid-state batteries.

■ ACKNOWLEDGMENTS

W.Z. and M.W. gratefully acknowledge financial support from the National Growth Fund program NXTGEN Hightech. A.K.L., M.T., and M.W. acknowledge the financial support from the 'BatteryNL − Next Generation Batteries based on Understanding Materials Interfaces' project NWA.1389.20.089 of the NWA research programme 'Research on Routes by Consortia (ORC)' funded by the Dutch Research Council (NWO). T.F. acknowledges the funding provided by the European Union's HORIZON EUROPE programme in the form of a Marie Skłodowska-Curie individual postdoctoral fellowship (project no. 101066486), and by the NWO in the form of an open-competition XS grant (OCENW.XS22.4.210).

■ REFERENCES

(1) Famprikis, T.; Canepa, P.; Dawson, J. A.; Islam, M. S.; Masquelier, C. Fundamentals of Inorganic Solid-State Electrolytes for Batteries. *Nat. Mater.* **2019**, *18* (12), 1278−1291.

(2) Randau, S.; Weber, D. A.; Kötz, O.; Koerver, R.; Braun, P.; Weber, A.; Ivers-Tiffée, E.; Adermann, T.; Kulisch, J.; Zeier, W. G.; Richter, F. H.; Janek, J. Benchmarking the Performance of All-Solid-State Lithium Batteries. *Nat. Energy* **2020**, *5* (3), 259−270.

(3) Liu, C.; Dai, H.; Wang, D.; Ren, X.; Lyu, S.; Fan, J.; Lv, S.; Zhu, S.; Li, N.; Wang, Y. Review—Understanding Thermal Runaway in Lithium-Ion Batteries: Trigger, Mechanism, and Early Warning Strategies. *J. Electrochem. Soc.* **2024**, *171* (12), 120527.

(4) Shahid, S.; Agelin-Chaab, M. A Review of Thermal Runaway Prevention and Mitigation Strategies for Lithium-Ion Batteries. *Energy Convers. Manag. X* **2022**, *16*, No. 100310.

(5) Tanaka, Y.; Ueno, K.; Mizuno, K.; Takeuchi, K.; Asano, T.; Sakai, A. New Oxyhalide Solid Electrolytes with High Lithium Ionic Conductivity > 10 mS cm^{-1} for All-Solid-State Batteries. *Angew. Chem., Int. Ed.* **2023**, *62* (13), No. e202217581.

(6) Ishiguro, Y.; Ueno, K.; Nishimura, S.; Iida, G.; Igarashib, Y. $TaCl_5$-Glassified Ultrafast Lithium Ion-Conductive Halide Electrolytes for High-Performance All-Solid-State Lithium Batteries. *Chem. Lett.* **2023**, *52* (4), 237−241.

(7) Feng, X.; Chien, P.-H.; Wang, Y.; Patel, S.; Wang, P.; Liu, H.; Immediato-Scuotto, M.; Hu, Y.-Y. Enhanced Ion Conduction by Enforcing Structural Disorder in Li-Deficient Argyrodites $Li_{6-x}PS_{5-x}Cl_{1+x}$. *Energy Storage Mater.* **2020**, *30*, 67−73.

(8) Gautam, A.; Al-Kutubi, H.; Famprikis, T.; Ganapathy, S.; Wagemaker, M. Exploring the Relationship Between Halide Substitution, Structural Disorder, and Lithium Distribution in Lithium Argyrodites ($Li_{6-x}PS_{5-x}Br_{1+x}$). *Chem. Mater.* **2023**, *35* (19), 8081−8091.

(9) Li, S.; Lin, J.; Schaller, M.; Indris, S.; Zhang, X.; Brezesinski, T.; Nan, C.; Wang, S.; Strauss, F. High-Entropy Lithium Argyrodite Solid Electrolytes Enabling Stable All-Solid-State Batteries. *Angew. Chem., Int. Ed.* **2023**, *62* (50), No. e202314155.

(10) Jung, W. D.; Kim, J.-S.; Choi, S.; Kim, S.; Jeon, M.; Jung, H.-G.; Chung, K. Y.; Lee, J.-H.; Kim, B.-K.; Lee, J.-H.; Kim, H. Superionic Halogen-Rich Li-Argyrodites Using In Situ Nanocrystal Nucleation and Rapid Crystal Growth. *Nano Lett.* **2020**, *20* (4), 2303−2309.

(11) Schwietert, T. K.; Arszelewska, V. A.; Wang, C.; Yu, C.; Vasileiadis, A.; de Klerk, N. J. J.; Hageman, J.; Hupfer, T.; Kerkamm, I.; Xu, Y.; van der Maas, E.; Kelder, E. M.; Ganapathy, S.; Wagemaker, M. Clarifying the Relationship between Redox Activity and Electrochemical Stability in Solid Electrolytes. *Nat. Mater.* **2020**, *19* (4), 428−435.

(12) Tan, D. H. S.; Wu, E. A.; Nguyen, H.; Chen, Z.; Marple, M. A. T.; Doux, J.-M.; Wang, X.; Yang, H.; Banerjee, A.; Meng, Y. S. Elucidating Reversible Electrochemical Redox of Li_6PS_5Cl Solid Electrolyte. *ACS Energy Lett.* **2019**, *4* (10), 2418−2427.

(13) Hu, L.; Wang, J.; Wang, K.; Gu, Z.; Xi, Z.; Li, H.; Chen, F.; Wang, Y.; Li, Z.; Ma, C. A Cost-Effective, Ionically Conductive and Compressible Oxychloride Solid-State Electrolyte for Stable All-Solid-State Lithium-Based Batteries. *Nat. Commun.* **2023**, *14* (1), 3807.

(14) Zhou, L.; Zuo, T.-T.; Kwok, C. Y.; Kim, S. Y.; Assoud, A.; Zhang, Q.; Janek, J.; Nazar, L. F. High Areal Capacity, Long Cycle Life 4 V Ceramic All-Solid-State Li-Ion Batteries Enabled by Chloride Solid Electrolytes. *Nat. Energy* **2022**, *7* (1), 83−93.

(15) Li, X.; Liang, J.; Chen, N.; Luo, J.; Adair, K. R.; Wang, C.; Banis, M. N.; Sham, T.; Zhang, L.; Zhao, S.; Lu, S.; Huang, H.; Li, R.; Sun, X. Water-Mediated Synthesis of a Superionic Halide Solid Electrolyte. *Angew. Chem., Int. Ed.* **2019**, *58* (46), 16427−16432.

(16) Xin, F.; Zhou, H.; Chen, X.; Zuba, M.; Chernova, N.; Zhou, G.; Whittingham, M. S. Li−Nb−O Coating/Substitution Enhances the Electrochemical Performance of the $LiNi_{0.8}Mn_{0.1}Co_{0.1}O_2$ (NMC 811) Cathode. *ACS Appl. Mater. Interfaces* **2019**, *11* (38), 34889−34894.

(17) Yu, P.; Zhang, H.; Hussain, F.; Luo, J.; Tang, W.; Lei, J.; Gao, L.; Butenko, D.; Wang, C.; Zhu, J.; Yin, W.; Zhang, H.; Han, S.; Zou, R.; Chen, W.; Zhao, Y.; Xia, W.; Sun, X. Lithium Metal-Compatible Antifluorite Electrolytes for Solid-State Batteries. *J. Am. Chem. Soc.* **2024**, *146* (18), 12681−12690.

(18) McDowell, M. T.; Lee, S. W.; Nix, W. D.; Cui, Y. 25th Anniversary Article: Understanding the Lithiation of Silicon and Other Alloying Anodes for Lithium-Ion Batteries. *Adv. Mater.* **2013**, *25* (36), 4966−4985.

(19) Zhu, Y.; He, X.; Mo, Y. Origin of Outstanding Stability in the Lithium Solid Electrolyte Materials: Insights from Thermodynamic Analyses Based on First-Principles Calculations. *ACS Appl. Mater. Interfaces* **2015**, *7* (42), 23685−23693.

(20) Ji, W.; Zheng, D.; Zhang, X.; Ding, T.; Qu, D. A Kinetically Stable Anode Interface for Li_3YCl_6-Based All-Solid-State Lithium Batteries. *J. Mater. Chem. A* **2021**, *9* (26), 15012−15018.

(21) Pang, Y.; Liu, Y.; Yang, J.; Zheng, S.; Wang, C. Hydrides for Solid-State Batteries: A Review. *Mater. Today Nano* **2022**, *18*, No. 100194.

(22) Gao, P.; Ju, S.; Xu, T.; Du, W.; Gao, Y.; Yang, Y.; Li, Z.; Zhang, H.; Huang, Y.; Xia, G.; Wang, F.; Yu, X. Hydrogen-Deficient Chain-Like Molecular Structure Confined Hydride Electrolyte for High-Voltage All-Solid-State Lithium Metal Batteries. *Adv. Mater.* **2025**, No. e08008. (Early view, Online Version of Record before inclusion in an issue.)

(23) Zhao, Y.; Daemen, L. L. Superionic Conductivity in Lithium-Rich Anti-Perovskites. *J. Am. Chem. Soc.* **2012**, *134* (36), 15042−15047.

(24) Li, W.; Li, M.; Chien, P.-H.; Wang, S.; Yu, C.; King, G.; Hu, Y.; Xiao, Q.; Shakouri, M.; Feng, R.; Fu, B.; Abdolvand, H.; Fraser, A.; Li, R.; Huang, Y.; Liu, J.; Mo, Y.; Sham, T.-K.; Sun, X. Lithium-Compatible and Air-Stable Vacancy-Rich $Li_9N_2Cl_3$ for High−Areal Capacity, Long-Cycling All−Solid-State Lithium Metal Batteries. *Sci. Adv.* **2023**, *9* (42), No. eadh4626.

(25) Landgraf, V.; Famprikis, T.; De Leeuw, J.; Bannenberg, L. J.; Ganapathy, S.; Wagemaker, M. Li_5NCl_2 : A Fully-Reduced, Highly-Disordered Nitride-Halide Electrolyte for Solid-State Batteries with Lithium-Metal Anodes. *ACS Appl. Energy Mater.* **2023**, *6* (3), 1661−1672.

(26) Landgraf, V.; Tu, M.; Zhao, W.; Lavrinenko, A. K.; Cheng, Z.; Canals, J.; de Leeuw, J.; Ganapathy, S.; Vasileiadis, A.; Wagemaker, M.; Famprikis, T. Disorder-Mediated Ionic Conductivity in Irreducible Solid Electrolytes. *J. Am. Chem. Soc.* **2025**, *147* (22), 18840−18852.

(27) Landgraf, V.; Tu, M.; Cheng, Z.; Vasileiadis, A.; Wagemaker, M.; Famprikis, T. Compositional Flexibility in Irreducible Antifluorite Electrolytes for Next-Generation Battery Anodes. *J. Mater. Chem. A* **2025**, *13* (5), 3562−3574.

https://doi.org/10.1021/acsenergylett.5c02289
ACS Energy Lett. 2025, 10, 5363−5372

(28) Szczuka, C.; Karasulu, B.; Groh, M. F.; Sayed, F. N.; Sherman, T. J.; Bocarsly, J. D.; Vema, S.; Menkin, S.; Emge, S. P.; Morris, A. J.; Grey, C. P. Forced Disorder in the Solid Solution Li_3P-Li_2S: A New Class of Fully Reduced Solid Electrolytes for Lithium Metal Anodes. *J. Am. Chem. Soc.* **2022**, *144* (36), 16350−16365.
(29) Li, W.; Li, M.; Wang, S.; Chien, P.-H.; Luo, J.; Fu, J.; Lin, X.; King, G.; Feng, R.; Wang, J.; Zhou, J.; Li, R.; Liu, J.; Mo, Y.; Sham, T.-K.; Sun, X. Superionic Conducting Vacancy-Rich β-Li_3N Electrolyte for Stable Cycling of All-Solid-State Lithium Metal Batteries. *Nat. Nanotechnol.* **2025**, *20* (2), 265−275.
(30) Sen, H. S.; Karasulu, B. Atomic-Level Insights into the Highly Conductive Lithium Thio-Phosphate Solid Electrolytes with Exceptional Stability against Lithium Metal. *J. Mater. Chem. A* **2025**, *13* (25), 19878−19895.
(31) Weppner, W.; Hartwig, P.; Rabenau, A. Consideration of Lithium Nitride Halides as Solid Electrolytes in Practical Galvanic Cell Applications. *J. Power Sources* **1981**, *6* (3), 251−259.
(32) Marx, R.; Lissner, F.; Schleid, T. Li_9NS_3 : Das erste Nitridsulfid der Alkalimetalle in einer Li_2 O-Typ-Variante. *Z. Für Anorg. Allg. Chem.* **2006**, *632* (12−13), 2151−2151.
(33) Wang, Z.; Xia, J.; Ji, X.; Liu, Y.; Zhang, J.; He, X.; Zhang, W.; Wan, H.; Wang, C. Lithium Anode Interlayer Design for All-Solid-State Lithium-Metal Batteries. *Nat. Energy* **2024**, *9* (3), 251−262.
(34) Zheng, J.; Perry, B.; Wu, Y. Antiperovskite Superionic Conductors: A Critical Review. *ACS Mater. Au* **2021**, *1* (2), 92−106.
(35) Ma, B.; Li, R.; Zhu, H.; Zhou, T.; Lv, L.; Zhang, H.; Zhang, S.; Chen, L.; Wang, J.; Xiao, X.; Deng, T.; Chen, L.; Wang, C.; Fan, X. Stable Oxyhalide-Nitride Fast Ionic Conductors for All-Solid-State Li Metal Batteries. *Adv. Mater.* **2024**, *36* (30), No. 2402324.
(36) Miara, L. J.; Suzuki, N.; Richards, W. D.; Wang, Y.; Kim, J. C.; Ceder, G. Li-Ion Conductivity in Li_9S_3N. *J. Mater. Chem. A* **2015**, *3* (40), 20338−20344.
(37) Li, S.; Yang, S.; Liu, G.; Hu, J.; Liao, Y.; Wang, X.; Wen, R.; Yuan, H.; Huang, J.; Zhang, Q. A Dynamically Stable Mixed Conducting Interphase for All-Solid-State Lithium Metal Batteries. *Adv. Mater.* **2024**, *36* (3), No. 2307768.
(38) Schwietert, T. K.; Vasileiadis, A.; Wagemaker, M. First-Principles Prediction of the Electrochemical Stability and Reaction Mechanisms of Solid-State Electrolytes. *JACS Au* **2021**, *1* (9), 1488−1496.
(39) Richards, W. D.; Miara, L. J.; Wang, Y.; Kim, J. C.; Ceder, G. Interface Stability in Solid-State Batteries. *Chem. Mater.* **2016**, *28* (1), 266−273.
(40) Nolan, A. M.; Zhu, Y.; He, X.; Bai, Q.; Mo, Y. Computation-Accelerated Design of Materials and Interfaces for All-Solid-State Lithium-Ion Batteries. *Joule* **2018**, *2* (10), 2016−2046.
(41) Hussain, F.; Zhu, J.; Zhao, Y.; Xia, W. Exploring Superionic Conduction in Lithium Oxyhalide Solid Electrolytes Considering Composition and Structural Factors. *Npj Comput. Mater.* **2024**, *10* (1), 148.
(42) van der Maas, E.; Zhao, W.; Cheng, Z.; Famprikis, T.; Thijs, M.; Parnell, S. R.; Ganapathy, S.; Wagemaker, M. Investigation of Structure, Ionic Conductivity, and Electrochemical Stability of Halogen Substitution in Solid-State Ion Conductor $Li_3YBr_xCl_{6-x}$. *J. Phys. Chem. C* **2023**, *127* (1), 125−132.
(43) Lee, T.; Joo, S.; Kang, S.; Kim, T.; Park, Y.; Chae, Y.; Kim, K.; Cho, W.; Kim, S. Multi-Solid-Electrolyte Systems for All-Solid-State Batteries: Current Status and Future Prospects. *ACS Appl. Energy Mater.* **2025**, *8* (9), 5585−5611.
(44) Lee, T.; Park, H.; Joo, S.; Kim, H.; Kim, J.; Kim, T.; Lee, W.; Kim, Y.; Kim, J.; Kim, K.; Cho, W.; Kim, S. Hydrogen-Rich Argyrodite Solid Electrolytes for NCM/Li All-Solid-State Batteries. *ACS Energy Lett.* **2024**, *9* (9), 4493−4500.
(45) Bai, C.; Li, Y.; Xiao, G.; Chen, J.; Tan, S.; Shi, P.; Hou, T.; Liu, M.; He, Y.-B.; Kang, F. Understanding the Electrochemical Window of Solid-State Electrolyte in Full Battery Application. *Chem. Rev.* **2025**, *125* (14), 6541−6608.
(46) Xu, H.; Li, Y.; Zhou, A.; Wu, N.; Xin, S.; Li, Z.; Goodenough, J. B. Li_3N-Modified Garnet Electrolyte for All-Solid-State Lithium Metal Batteries Operated at 40 °C. *Nano Lett.* **2018**, *18* (11), 7414−7418.
(47) Zhang, Y.; Chang, H.; Han, A.; Xu, S.; Wang, X.; Yang, S.; Hu, X.; Sun, Y.; Sun, X.; Chen, X.; Yang, Y. Synergistic Li_6PS_5Cl@Li_3OCl Composite Electrolyte for High-Performance All-Solid-State Lithium Batteries. *Green Energy Environ* **2025**, *10* (4), 793−803.
(48) Shen, L.; Wang, Z.; Xu, S.; Law, H. M.; Zhou, Y.; Ciucci, F. Harnessing Database-Supported High-Throughput Screening for the Design of Stable Interlayers in Halide-Based All-Solid-State Batteries. *Nat. Commun.* **2025**, *16* (1), 3687.
(49) Wang, Z.; Wang, T.; Zhang, N.; Zhang, W.; Liu, Y.; Wang, C. Interlayer Design for Halide Electrolytes in All-Solid-State Lithium Metal Batteries. *Adv. Mater.* **2025**, *37*, No. 2501838.
(50) Xu, X.; Du, G.; Cui, C.; Liang, J.; Zeng, C.; Wang, S.; Ma, Y.; Li, H. Stabilizing the Halide Solid Electrolyte to Lithium by a β-Li_3N Interfacial Layer. *ACS Appl. Mater. Interfaces* **2022**, *14* (35), 39951−39958.
(51) Deysher, G.; Oh, J. A. S.; Chen, Y.-T.; Sayahpour, B.; Ham, S.-Y.; Cheng, D.; Ridley, P.; Cronk, A.; Lin, S. W.-H.; Qian, K.; Nguyen, L. H. B.; Jang, J.; Meng, Y. S. Design Principles for Enabling an Anode-Free Sodium All-Solid-State Battery. *Nat. Energy* **2024**, *9*, 1611−1672.
(52) Galvez-Aranda, D. E.; Seminario, J. M. Ab Initio Study of the Interface of the Solid-State Electrolyte $Li_9N_2Cl_3$ with a Li-Metal Electrode. *J. Electrochem. Soc.* **2019**, *166* (10), A2048−A2057.
(53) Zhu, Y.; Mo, Y. Materials Design Principles for Air-Stable Lithium/Sodium Solid Electrolytes. *Angew. Chem., Int. Ed.* **2020**, *59* (40), 17472−17476.
(54) Morino, Y.; Ito, D.; Otoyama, M.; Gamo, H.; Kato, M.; Takeichi, N.; Sano, H. Moisture Stability of Sulfide Solid Electrolytes: Systematic Comparison and Mechanistic Insight. *Electrochemistry* **2025**, *93* (6), 063001−063001.
(55) Zhang, J.; Hu, Y. H. Higher Chemical Stability of α-Li_3N than β-Li_3N in Atmosphere. *Top. Catal.* **2015**, *58* (4−6), 386−390.
(56) Nazri, G. Preparation, Structure and Ionic Conductivity of Lithium Phosphide. *Solid State Ion* **1989**, *34* (1−2), 97−102.
(57) Li, W.; Li, M.; Ren, H.; Kim, J. T.; Li, R.; Sham, T.-K.; Sun, X. Nitride Solid-State Electrolytes for All-Solid-State Lithium Metal Batteries. *Energy Environ. Sci.* **2025**, *18* (10), 4521−4554.
(58) de Klerk, N. J. J.; Roslon, T.; Wagemaker, M. Diffusion Mechanism of Li Argyrodite Solid Electrolytes for Li-Ion Batteries and Prediction of Optimized Halogen Doping: The Effect of Li Vacancies, Halogens, and Halogen Disorder. *Chem. Mater.* **2016**, *28* (21), 7955−7963.
(59) Asano, T.; Sakai, A.; Ouchi, S.; Sakaida, M.; Miyazaki, A.; Hasegawa, S. Solid Halide Electrolytes with High Lithium-Ion Conductivity for Application in 4 V Class Bulk-Type All-Solid-State Batteries. *Adv. Mater.* **2018**, *30* (44), No. 1803075.
(60) Wu, J.; Yuan, L.; Zhang, W.; Li, Z.; Xie, X.; Huang, Y. Reducing the Thickness of Solid-State Electrolyte Membranes for High-Energy Lithium Batteries. *Energy Environ. Sci.* **2021**, *14* (1), 12−36.
(61) Surendran, V.; Thangadurai, V. Solid-State Lithium Metal Batteries for Electric Vehicles: Critical Single Cell Level Assessment of Capacity and Lithium Necessity. *ACS Energy Lett.* **2025**, *10* (2), 991−1001.
(62) Oh, J.; Choi, S. H.; Kim, H.; Chung, W. J.; Kim, M.; Kim, I.; Lee, T.; Lee, J.; Kim, D. O.; Moon, S.; Kim, D.; Choi, J. W. Solvent−Binder Engineering for a Practically Viable Solution Process for Fabricating Sulfide-Based All-Solid-State Batteries. *ACS Energy Lett.* **2025**, *10*, 2831−2838.
(63) Choi, S.; Ann, J.; Do, J.; Lim, S.; Park, C.; Shin, D. Application of Rod-Like Li_6 PS_5 Cl Directly Synthesized by a Liquid Phase Process to Sheet-Type Electrodes for All-Solid-State Lithium Batteries. *J. Electrochem. Soc.* **2019**, *166* (3), A5193−A5200.
(64) Li, D.; Liu, H.; Wang, C.; Yan, C.; Zhang, Q.; Nan, C.; Fan, L. High Ionic Conductive, Mechanical Robust Sulfide Solid Electrolyte Films and Interface Design for All-Solid-State Lithium Metal Batteries. *Adv. Funct. Mater.* **2024**, *34* (27), No. 2315555.
(65) Kim, C.; Li, Y.; Jang, I.; Wu, W.; Su, Y.; Meyer, H. M.; Keum, J.; Nanda, J.; Yang, G. Pushing the Limits: Maximizing Energy Density in Silicon Sulfide Solid-State Batteries. *Adv. Mater.* **2025**, *37*, No. 2502300.

https://doi.org/10.1021/acsenergylett.5c02289
ACS Energy Lett. 2025, 10, 5363−5372

(66) Zhang, H.; Qiu, J.; Pang, J.; Cao, G.; Zhang, B.; Wang, L.; He, X.; Feng, X.; Ma, S.; Zhang, X.; Ming, H.; Li, Z.; Li, F.; Zhang, H. Sub-Millisecond Lithiothermal Synthesis of Graphitic Meso−Microporous Carbon. *Nat. Commun.* **2024**, *15* (1), 3491.
(67) Kozen, A. C.; Lin, C.-F.; Pearse, A. J.; Schroeder, M. A.; Han, X.; Hu, L.; Lee, S.-B.; Rubloff, G. W.; Noked, M. Next-Generation Lithium Metal Anode Engineering *via* Atomic Layer Deposition. *ACS Nano* **2015**, *9* (6), 5884−5892.
(68) Tu, M.; Landgraf, V.; Zhao, W.; Cheng, Z.; Famprikis, T.; Wang, X.; Ganapathy, S.; Wagemaker, M. Highly-Conductive Irreducible Electrolytes for next Generation Low-Potential Anodes. *ChemRxiv (Preprint)*. July 17, **2025**.
(69) Xu, Q.; Li, T.; Ju, Z.; Chen, G.; Ye, D.; Waterhouse, G. I. N.; Lu, Y.; Lai, X.; Zhou, G.; Guo, L.; Yan, K.; Tao, X.; Li, H.; Qiu, Y. Li_2ZrF_6-Based Electrolytes for Durable Lithium Metal Batteries. *Nature* **2025**, *637* (8045), 339−346.
(70) Peng, L.; Chen, S.; Yu, C.; Wei, C.; Liao, C.; Wu, Z.; Wang, H.-L.; Cheng, S.; Xie, J. Enhancing Moisture and Electrochemical Stability of the $Li_{5.5}PS_{4.5}Cl_{1.5}$ Electrolyte by Oxygen Doping. *ACS Appl. Mater. Interfaces* **2022**, *14* (3), 4179−4185.
(71) Aimi, A.; Onodera, H.; Shimonishi, Y.; Fujimoto, K.; Yoshida, S. High Li-Ion Conductivity in Pyrochlore-Type Solid Electrolyte $Li_{2-x}La_{(1+x)/3}M_2O_6F$ (M = Nb, Ta). *Chem. Mater.* **2024**, *36* (8), 3717−3725.
(72) Battery Electrodes, Electrolytes, and Their Interfaces. In *Handbook of Materials Modeling*; Springer International Publishing: Cham, 2018; pp 1−24. DOI: 10.1007/978-3-319-50257-1_96-1.
(73) Chen, C.; Nguyen, D. T.; Lee, S. J.; Baker, N. A.; Karakoti, A. S.; Lauw, L.; Owen, C.; Mueller, K. T.; Bilodeau, B. A.; Murugesan, V.; Troyer, M. Accelerating Computational Materials Discovery with Machine Learning and Cloud High-Performance Computing: From Large-Scale Screening to Experimental Validation. *J. Am. Chem. Soc.* **2024**, *146* (29), 20009−20018.
(74) Dutra, A. C. C.; Dawson, J. A. Computational Design of Antiperovskite Solid Electrolytes. *J. Phys. Chem. C* **2023**, *127* (37), 18256−18270.
(75) Jacobs, R.; Morgan, D.; Attarian, S.; Meng, J.; Shen, C.; Wu, Z.; Xie, C. Y.; Yang, J. H.; Artrith, N.; Blaiszik, B.; Ceder, G.; Choudhary, K.; Csanyi, G.; Cubuk, E. D.; Deng, B.; Drautz, R.; Fu, X.; Godwin, J.; Honavar, V.; Isayev, O.; Johansson, A.; Kozinsky, B.; Martiniani, S.; Ong, S. P.; Poltavsky, I.; Schmidt, K.; Takamoto, S.; Thompson, A. P.; Westermayr, J.; Wood, B. M. A Practical Guide to Machine Learning Interatomic Potentials − Status and Future. *Curr. Opin. Solid State Mater. Sci.* **2025**, *35*, No. 101214.
(76) Xu, S.; Wu, J.; Guo, Y.; Zhang, Q.; Zhong, X.; Li, J.; Ren, W. Applications of Machine Learning in Surfaces and Interfaces. *Chem. Phys. Rev.* **2025**, *6* (1), No. 011309.
(77) Sun, Z.; Li, X.; Wu, Y.; Gu, Q.; Zheng, S. Machine Learning-Assisted Simulations and Predictions for Battery Interfaces. *Adv. Intell. Syst.* **2025**, *7*, No. 2400626.

https://doi.org/10.1021/acsenergylett.5c02289
ACS Energy Lett. 2025, 10, 5363−5372